SARS-CoV-2 Infection and Transmission Depends on Heparan Sulfates and Is Blocked by Low Molecular Weight Heparins

Marta Bermejo-Jambrina[1†], Julia Eder[1†], Tanja M. Kaptein[1], Leanne C. Helgers[1], Philip J.M. Brouwer[2], John L. van Hamme[1], Alexander P.J. Vlaar[3], Frank E.H.P. van Baarle[3], Godelieve J. de Bree[4], Bernadien M. Nijmeijer[1], Neeltje A. Koostra[1], Marit J. van Gils[2], Rogier W. Sanders[2,5], Teunis B. H. Geijtenbeek[1*]

[1]Department of Experimental Immunology, Amsterdam institute for Infection and Immunity, Amsterdam University Medical Centers, University of Amsterdam, Meibergdreef 9, Amsterdam, The Netherlands.
[2]Department of Medical Microbiology, Amsterdam institute for Infection and Immunity, Amsterdam University Medical Centers, University of Amsterdam, Meibergdreef 9, Amsterdam, The Netherlands.
[3]Department of Intensive Care Medicine, Amsterdam University Medical Centers, University of Amsterdam, Meibergdreef 9, Amsterdam, The Netherlands.
[4]Department of Internal Medicine, Amsterdam institute for Infection and Immunity, Amsterdam University Medical Centers, University of Amsterdam, Meibergdreef 9, Amsterdam, The Netherlands.
[5]Department of Microbiology and Immunology, Weill Medical College of Cornell University, New York, NY 10021, USA.

* Corresponding author:
Prof. dr. Teunis B.H. Geijtenbeek, phone: +31 (0)20 56 66063, email: t.b.geijtenbeek@amsterdamumc.nl, Department of Experimental Immunology, Amsterdam University Medical Centers, location AMC, University of Amsterdam, Meibergdreef 9, 1105 AZ, Amsterdam, The Netherlands

† These authors contributed equally.

Keywords: SARS-CoV-2, Syndecans, attachment block, inhibit infection, epithelial cells

Abstract

The current pandemic caused by severe acute respiratory syndrome coronavirus-2 (SARS-CoV-2) and new outbreaks worldwide highlight the need for preventive treatments. Although angiotensin converting enzyme 2 (ACE2) is the primary receptor for SARS-CoV-2, we identified heparan sulfate proteoglycans expressed by epithelial cells, alveolar macrophages and dendritic cells as co-receptors for SARS-CoV-2. Low molecular weight heparins (LMWH) blocked SARS-CoV-2 infection of epithelial cells and alveolar macrophages, and virus dissemination by dendritic cells. Notably, potent neutralizing antibodies from COVID-19 patients interfered with SARS-CoV-2 binding to heparan sulfate proteoglycans, underscoring the importance of heparan sulfate proteoglycans as receptors and uncover that SARS-CoV-2 binding to heparan sulfates is an important mechanism for neutralization. These results have imperative implications for our understanding of SARS-CoV-2 host cell entry and reveal an important target for novel prophylactic intervention.

Introduction

Severe acute respiratory syndrome coronavirus 2 (SARS-CoV-2) emerged in Wuhan, China in late 2019 and can cause coronavirus disease 2019 (COVID-19), an influenza-like disease ranging from mild respiratory symptoms to severe lung injury, multi organ failure and death (1-3). SARS-CoV-2 spread quickly and has caused a pandemic with a severe impact on global health and world economy (4, 5). SARS-CoV-2 is transmitted predominantly via large droplets expelled from the upper respiratory tract through sneezing and coughing (6, 7) and is subsequently taken up via mucosal surfaces of the nose, mouth and eyes (8). SARS-CoV-2 infects epithelial cells in the respiratory tract, such as ciliated mucus secreting bronchial epithelial cells and type 1 pneumocytes in the lung, as well as epithelial cells in the gastrointestinal tract (9, 10). To date, there is no treatment to prevent SARS-CoV-2 infection. Lockdown strategies and social distancing mitigate viral spread but due to negative socioeconomic consequences these are not feasible long-term solutions (11, 12). Recent renewed outbreaks underscore the urgent need for protective strategies specifically targeting SARS-CoV-2 to prevent further dissemination.

SARS-CoV-2 belongs to the betacoronaviruses, a family that also includes SARS-CoV and MERS-CoV (13). The coronavirus Spike (S) protein is a class I fusion protein that mediates virus entry (14, 15). The S protein consist of two subunits; S1 directly engages via its receptor-binding domain (RBD) with host surface receptors (16, 17) and S2 mediates fusion between virus and cell membrane (18, 19). SARS-CoV-2 uses angiotensin-converting enzyme 2 (ACE2) as its main receptor (13, 20). ACE2 is a type I integral membrane protein abundantly expressed on epithelial cells lining the respiratory tract (21) but also the ileum, esophagus and liver (22) and ACE2 expression dictates SARS-CoV-2 tropism (10). However, it remains unclear whether SARS-CoV2 requires other receptors for virus entry. Neutralizing monoclonal antibodies against SARS-CoV-2 have been identified that are directed not only at the RBD but also outside the RBD (23), supporting the presence of other receptors. Here we show that the heparan sulfate proteoglycans (HSPG) Syndecan 1 and 4 are required for SARS-CoV-2 infection of permissive cells, and that low molecular weight heparins (LMWH) efficiently inhibited infection of polarized epithelial cells as well as alveolar macrophages. Moreover, we show that primary DC subsets use HSPG as attachment receptors to facilitate dissemination of

SARS-CoV-2. These findings are important to develop prophylactics against SARS-CoV-2 or prevent dissemination early after infection.

Results

Heparan sulfate proteoglycans are crucial for SARS-CoV-2 binding and infection

Heparan sulfates are expressed by most cells including epithelial cells as heparan sulfate proteoglycans and these have been shown to interact with viruses such as HIV-1, HCV, Sindbis virus and also SARS-CoV (24-28). We incubated Huh 7.5 cells that express ACE2 (Supplementary Fig. 1A) with SARS-CoV-2 pseudovirus (23) and observed strong binding of SARS-CoV-2 pseudovirus to cells (Fig. 1A). Binding of SARS-CoV-2 was inhibited by a blocking antibody against ACE2 (Fig. 1A). Moreover, SARS-CoV-2 pseudovirus binding was inhibited by neutralizing antibodies from COVID-19 patients directed against the RBD (COVA1-18, COVA2-15) and non-RBD (COVA1-21) epitopes of the SARS-CoV-2 S protein (23). Notably, unfractionated (UF) heparin potently inhibited the binding of SARS-CoV-2 pseudovirus to cells comparable to the antibody against ACE2 (Fig. 1B). Enzymatic removal of heparan sulfates on the cell surface by Heparinase treatment decreased SARS-CoV-2 virus binding (Fig. 1C and Supplementary Fig. 1B). Furthermore, we observed that SARS-CoV-2 pseudovirus infected Huh 7.5 cells, which was blocked by UF heparin (Fig. 1D). These data strongly suggest that SARS-CoV-2 requires heparan sulfates to infect ACE2-positive cells.

Low molecular weight heparins inhibit SARS-CoV-2 infection

Low molecular weight heparin (LMWH) have replaced UF heparin in the clinic as anti-coagulant treatment due to their smaller size and superior pharmacological properties (29) Importantly, LMWH therapy has recently been shown to decrease mortality in severely ill COVID-19 patients (30) and is now used as anti-coagulant prophylaxis for COVID-19 patients. Several LMWH are used clinically and differ in size and preparation (31). We therefore screened different LMWHs for their ability to block SARS-CoV-2 binding and infection. All LMWH tested blocked SARS-CoV-2 binding to Huh 7.5 cells and inhibition was similar to that of UF heparin (Fig. 2A). Moreover, the different LMWH inhibited infection of Huh 7.5 cells with SARS-CoV-2 pseudovirus in a dose dependent manner

(Fig. 2B). Thus, we have identified LMWH as inhibitors of SARS-CoV-2 binding and infection.

SARS-CoV-2 infection of epithelial cells is blocked by UF heparin and LMWH

Human kidney epithelial 293T cells with ectopic expression of ACE2 have been used by different studies to investigate the role of ACE2 in SARS-CoV-2 infection ((20, 32) and Supplementary Fig. 1C). Ectopic expression of ACE2 on 293T cells rendered these cells susceptible to SARS-CoV-2 pseudovirus infection but infection was abrogated by both LMWH enoxaparin and UF heparin to a similar level as antibodies against ACE2 (Fig. 3A). The combination of ACE2 antibodies and LMWH enoxaparin or UF heparin fully blocked infection of 293T-ACE2 cells (Fig. 3A). These data strongly suggest that heparan sulfates play a crucial role in SARS-CoV-2 infection.

Epithelial cells expressing ACE2 are thought to be primary target cells for SARS-CoV-2 infection in the lung and intestinal tract (21, 33). Non-polarized human colon carcinoma Caco-2 cells efficiently bound SARS-CoV-2 pseudovirus (Fig. 3B). Treatment with antibodies against ACE2, UF heparin and LMWH enoxaparin blocked virus binding to the epithelial cell line. Non-polarized epithelial cells express low levels of ACE2 ((34) and Supplementary Fig. 1C) and Caco2 cells were infected by SARS-CoV-2 pseudovirus albeit at a low level. LMWH enoxaparin blocked infection of Caco2 cells similar as antibodies against ACE2 (Fig. 3C). Combining ACE2 antibodies with UF heparin or LMWH enoxaparin did not further increase block in non-polarized Caco2 (Fig. 3B and C). Next we cultured Caco-2 cells on a microporous filter and infected the cells with SARS-CoV-2 pseudovirus once they had formed a highly polarized epithelial monolayer. The polarized Caco-2 cells were permissive to infection, which was significantly blocked by LMWH treatment to a similar level as antibodies against ACE2 (Fig. 3D). The combination of an antibody against ACE2 together with LMWH enoxaparin showed the same pattern as each treatment independently (Fig. 3D). These data suggest that heparan sulfates are required for SARS-CoV-2 infection of (non-)polarized epithelial cells.

Heparan sulfates are required for transmission by primary dendritic cells

SARS-CoV-2 infects cells in nasal mucosa, lung and the intestinal tract but mechanisms for dissemination of the virus from the respiratory and intestinal tract are still unclear. It has been suggested that macrophages become infected by SARS-CoV-2 (35), which

might promote dissemination. Notably, alveolar macrophages isolated by bronchoalveolar lavage were infected by SARS-CoV-2 (Fig 4A). Importantly, LMWH enoxaparin inhibited infection of primary alveolar macrophages with SARS-CoV-2 (Fig. 4A).Different dendritic cell (DC) subsets have been shown to be involved in dissemination of various viruses including SARS-CoV (36-38). We differentiated monocytes to DC, which is a model for submucosal DC, and also isolated primary human Langerhans cells (LCs) from skin (39, 40) as this DC subset resides in epidermis of skin and squamous mucosa of different tissues (41). Both DC and LC efficiently bound SARS-CoV-2 pseudovirus and binding was inhibited by UF heparin as well as LMWH enoxaparin (Fig. 4B and C). Neither DC nor LC expressed ACE2 (Supplementary Fig. 1A) and, SARS-CoV-2 pseudovirus did not infect DC nor LC (Fig. 4D and E). However, DC subsets are able to transmit HIV-1 to target cells independent of productive infection (40, 42). We therefore treated DC and LC with SARS-CoV-2 pseudovirus and after washing co-cultured the cells with susceptible Huh 7.5 cells. Notably, both DCs and LCs efficiently transmitted captured SARS-CoV-2 to Huh 7.5 cells and transmission was blocked by UF heparin as well as LMWH enoxaparin pre-treatment (Fig. 4F and G). Thus, our data strongly suggest that DC subsets are involved in virus dissemination of SARS- CoV-2 independent of direct infection and in a heparan sulfate-dependent manner.

Heparan sulfate proteoglycans Syndecan 1 and 4 are important for SARS-CoV-2 binding and infection

The heparan sulfate proteoglycan family of Syndecans are particularly important in facilitating cell adhesion of several viruses (28, 43). Therefore we investigated SARS-CoV-2 binding to Namalwa cells expressing Syndecan 1 and 4 (Supplementary Fig. 2A) as these Syndecans are expressed by epithelial cells (44, 45). Namalwa cells did not express ACE2 (Supplementary Fig. 1A). SARS-CoV-2 pseudovirus bound to Syndecan 1 and 4 transduced cell-lines with higher efficiency than the parental cell-line (Fig. 5A and (Supplementary Fig. 2A). UF heparin and LMWH enoxaparin blocked the interaction of Syndecan 1 and 4 with SARS-CoV-2 pseudovirus (Fig. 5A).

Epithelial cells (44, 45) and Huh 7.5 cells express Syndecan 1 and 4 and we silenced both Syndecan 1 and 4 by RNA interference (Supplementary Fig. 2B). Notably, silencing of Syndecan 1 or Syndecan 4 decreased SARS-CoV-2 infection of Huh 7.5 cells (Fig. 5B) supporting a role for Syndecan 1 and 4 in SARS-CoV-2 infection. These data indicate that

Syndecan 1 and 4 are the main heparan sulfate proteoglycans involved in SARS-CoV-2 binding and infection.

Potent neutralizing antibodies against SARS-CoV-2 S protein target heparan sulfate-SARS-CoV-2 interactions

Recently several potent neutralizing antibodies against SARS-CoV-2 have been isolated from COVID-19 patients that target the RBD (COVA1-15, COVA1-18) as well as the non-RBD (COVA1- 21) of the S protein (23). In order to investigate whether these antibodies can prevent binding of SARS-CoV-2 to heparan sulfates, we examined their ability to inhibit virus binding to ACE2-negative Namalwa cells expressing Syndecan 1. Notably, the two RBD and the non-RBD binding antibodies blocked the interaction of SARS-CoV-2 pseudovirus with Syndecan 1 to a similar extent as LMWH (Fig. 6A). In contrast, the isotype antibodies did not inhibit virus binding.

To investigate whether these antibodies specifically block the interaction of SARS-CoV-2 with heparan sulfates, we coated UF heparin and measured SARS-CoV-2 S protein binding. SARS- CoV-2 S protein efficiently bound to coated heparin (Fig. 6B). All three antibodies against S protein blocked the interaction of heparin with SARS-CoV-2, strongly suggesting that the neutralizing antibodies against SARS-CoV-2 interfere with heparan sulfate binding by the virus. Thus, our data strongly suggest that neutralization by antibodies against SARS-CoV-2 can occur via ACE2 inhibition but also by preventing SARS-CoV-2 binding to heparan sulfate proteoglycans, and underscores the importance of heparan sulfate proteoglycans in infection.

Discussion

Here we have shown that SARS-CoV-2 infection is not only dependent on ACE2 but also requires heparan sulfate proteoglycans and in particular Syndecan 1 and 4. Our data suggest that SARS-CoV-2 attaches to cells via HSPG, which facilitates thereby interaction with ACE2 and subsequent infection. Moreover, we also identified HSPG as important receptors facilitating ACE2-independent transmission by primary DCs. Infection as well as transmission with SARS-CoV-2 was efficiently inhibited by the clinically adapted UF heparin and LMWH. It further suggests that neutralizing antibodies isolated from COVID-19 patients could at least partially inhibit SARS- CoV- 2 binding to heparan sulfate

proteoglycans and thereby interfere with infection. These results have important implications for our understanding of SARS-CoV-2 host cell entry and reveal a relevant target for novel prophylactic intervention.

Recently, is has been suggested that the SARS-CoV-2 S protein interacts with heparan sulfate molecules and heparin (46-48). Here we have identified heparan sulfates and in particular Syndecan 1 and 4 as important receptors for SARS-CoV-2. Our data strongly suggest that the heparan sulfate proteoglycans are required for virus binding and infection of epithelial cells. LMWH or UF heparin efficiently abrogated virus infection to a similar extent as ACE2 antibodies and combinations of ACE2 antibodies, suggesting that both receptors are required for virus infection. To investigate the role of SARS-CoV-2 infection in primary cells, we isolated alveolar macrophages and epidermal LCs, and cultured monocyte-derived DCs. Interestingly, alveolar macrophages were infected by SARS-CoV-2 in a HSPG dependent manner whereas neither LCs nor DCs were infected. The role of alveolar macrophages in SARS-CoV-2 infection is still unclear but it has been hypothesized that they can infiltrate other tissues or induce pro-inflammatory cytokines and chemokines upon infection (49), indicating a potential detrimental role in disease progression. Interestingly, infection of primary alveolar macrophages isolated from lung was also inhibited by LMWH, suggesting an important role for LMWH protection in lung tissue not as an anti-coagulant but as an antiviral.

DCs migrate from mucosal tissues and epidermis into lymphoid tissues (50) and therefore it is thought that DCs are involved in the dissemination of viruses after infection (51). Our data strongly suggest that DCs similarly are involved in SARS-CoV-2 dissemination via HSPG as primary DC subsets isolated from skin or derived from blood monocytes strongly bound SARS-CoV-2 via HSPG and efficiently transmitted the virus to target epithelial cells. The HSPG cell surface receptor primarily expressed by epithelial cells is Syndecan 1 (44, 52) and is involved in cell recruitment, proliferation and inflammations (45) but can also bind viruses like Herpes simplex virus (HSV-1) (43) and Hepatitis C virus (53). Syndecan 4 is further expressed ubiquitously albeit at lower levels (45). Recently we could show that Syndecan 4 is involved in transmission of HCV by LCs (28) whereas Syndecan 3 facilitates binding and transmission of HIV-1 (54). In this study we demonstrate the interaction of specific Syndecans with SARS-CoV-2 and underscore their importance for virus attachment and dissemination.

Neutralizing antibodies against SARS-CoV-2 are a potential therapy for COVID-19 patients and several potent monoclonal neutralizing antibodies have been identified that target the RBD and non-RBD sites of the S protein of SARS-CoV-2 (23). However, while most of the antibodies are suggested to inhibit ACE2 binding sites, the non-RBD antibodies COVA1-21 does not seem to interfere with ACE2 and instead interfere with other COVA antibodies and as yet unidentified receptors. Notably, two RBD antibodies COVA1-18 and COVA2-15 blocked virus as well as S protein binding to heparan sulfates, indicating that the RBD is also involved in heparan sulfate interactions (23). Moreover, our data suggest that COVA1-21 targets the heparan binding site of the S protein. Recent studies suggest that the heparan sulfate binding site of the S protein are outside the RBD of SARS-CoV-2 (47, 48). The finding that neutralizing antibodies against SARS-CoV-2 block heparan sulfate interactions suggest that this is an important target for neutralization of the and underscores the importance of the interaction for SARS-CoV-2 infection. Thus this finding shows that the unusually potent antibodies COVA1-18 and 2-15 can neutralize SARS-CoV-2 through two mechanisms: preventing SARS-CoV-2 binding to ACE2 (23) and to heparan sulfate proteoglycans.

LMWHs are already used as subcutaneous treatment of COVID-19 patients to prevent systemic clotting (55, 56). Interestingly, here we have identified an important ability of LMWH to directly block SARS-CoV-2 binding and infection of epithelial cells as well as preventing virus transmission. Our data support the use of LMWH as prophylactic treatment for SARS-CoV-2 as well as a treatment option early in infection to block further infection and dissemination. LMWH inhalation has been studied to attenuate inflammatory responses in COPD and asthma patients and is considered safe to use as a prophylactic. The clinical use of LMWH to treat COVID-19 and our finding that LMWH block virus infection and dissemination strongly advocate for the prophylactic use of LMWH in individuals at risk for infection, or short after infection or even for a general population during outbreaks we still observe daily to quickly limit transmission events.

In summary, this study provided new insights into how SARS-CoV-2 initiates attachment, infection and transmission in different cell types and showed that LMWH are possible candidates for prophylactic intervention and antiviral treatment.

Materials and Methods

Virus production

For production of single-round infection viruses, human embryonic kidney 293T/17 cells (ATCC, CRL-11268) were co-transfected with an adjusted HIV backbone plasmid (pNL4-3.Luc.R-S-) containing previously described stabilizing mutations in the capsid protein (PMID: 12547912) and firefly luciferase in the *nef* open reading frame (1.35ug) and pSARS-CoV-2 expressing SARS-CoV-2 S protein (0.6ug) (GenBank; MN908947.3) (23). Transfection was performed in 293T/17 cells using genejuice (Novagen, USA) transfection kit according to manufacturer's protocol. At day 3 or day 4, pseudotyped SARS-CoV-2 virus particles were harvested and filtered over a 0.45 µm nitrocellulose membrane (SartoriusStedim, Gottingen, Germany).

SARS-CoV-2 pseudovirus productions were quantified by p24 ELISA (Perkin Elmer Life Sciences).

Reagents and antibodies

The following antibodies were used (all anti-human): ACE-2 (R&D), (Heparan Sulfate (clone F58-10E4) (Amsbio), digested Heparan (clone F69-3G10) (Amsbio), CD1a-APC mouse IgG1 (BD Biosciences, San Jose, CA, USA), CD207-PE (langerin) mouse IgG1 (#IM3577) FITC-conjugated goat-anti-mouse IgM (#31992) (Invitrogen), AF488-conjugated donkey-anti-mouse IgG2b (Invitrogen), Flow cytometric analyses were performed on a BD FACS Canto II (BD Biosciences). Data was analyzed using FlowJo vX.0.7 software (TreeStar).

The following reagents were used: Unfractionated (UF) heparin, 5.000 I.E./ml (LEO). Low Molecular Weight heparins (LMWH): dalteparin, 10.000 IE anti-Xa/ml (Pfizer), tinzaparin, 10.000 IE anti-X1/0.5ml (LEO), enoxaparin, 6000 IE (60mg)/0.6 ml (Sanofi), nadroparin, 9.500 IE anti-XA/ml (Aspen). Heparinase III from *Flavobacterium heparium*, EC 4.2.2.8, Batch 010, (Amsbio). Biotinylated SARS-CoV-2 S protein as well as neutralizing antibodies COVA1-18, COVA-1-21 and COVA-2-15 were generated as described previously (23).

Cell lines

The human B cell line Namalwa (ATCC, CRL-1432) and Namalwa cells stably expressing human Syndecan 1 and Syndecan 4 (57) were a gift from Dr. Guido David and Dr. Philippe A Gallay. The cells were maintained in RPMI 1640 medium (Gibco Life Technologies, Gaithersburg, Md.) containing 10% fetal calf serum (FCS), penicillin/streptomycin (10 µg/ml) and 1 mM sodium pyruvate (Thermo Fisher). The expression of the different Syndecans was validated by PCR analysis using specific primers aimed against Syndecans. Huh7.5 (human hepatocellular carcinoma) cells received from dr. Charles M. Rice (58) were maintained in Dulbecco modified Eagle medium (Gibco Life Technologies, Gaithersburg, Md.) containing 10% fetal calf serum (FCS), L-glutamine and penicillin/streptomycin (10 µg/ml). Medium was supplemented with 1mM Hepes buffer (Gibco Life Technologies, Gaithersburg, Md.). The human embryonic kidney 293T/17 cells (ATCC, CRL-11268) were maintained in maintained in Dulbecco modified Eagle medium (Gibco Life Technologies, Gaithersburg, Md.) containing 10% fetal calf serum (FCS), L-glutamine and penicillin/streptomycin (10 µg/ml). The human epithelial Caco2 cells (ATCC, HTB-37™) were maintained in Dulbecco modified Eagle medium (Gibco Life Technologies, Gaithersburg, Md.) containing 10% fetal calf serum (FCS), L-glutamine and penicillin/streptomycin (10 µg/ml) and supplemented with MEM Non-Essential Amino Acids Solution (NEAA) (Gibco Life Technologies, Gaithersburg, Md.). To create a monolayer of polarized cells, Caco2 cells were maintained in 6.5 mm transwells with a 5 µm Pore Polycarbonate Membrane Insert (Corning). The cells were initially seeded with a density of 25.000 cells per 6.5 mm filter insert and full polarization was reached after 4 weeks in culture.

SARS-CoV-2 S protein binding ELISA

UF Heparin (diluted in PBS) was coated using high binding ELISA plates for 2h at 37°C. Non-specific binding was blocked by incubating the plate 1% BSA in TSM (20 mM Tris–HCl, pH 7.4, containing 150 mM NaCl, 2 mM CaCl2, and 2 mM MgCl2) for 30 min at 37 °C. Biotinylated Spike protein was pre-incubated with different antibodies (20 µg/ml) for 30 min at RT. Biotinylated SARS-CoV-2 S protein was added for 2 hours at RT. Unbound Spike protein was washed away and streptavidin-HRP (1/10000) (Thermofisher) was added. After washing, a TMB/hydrogen peroxide substrate was added for color development. This reaction was stopped by adding 0.8 M H2SO4 and the optical density

was measured at 450 nm. Negative control included isotype-matched HIV-1 antibody VRC01 (59).

293T Transfection with ACE2

To generate cells expressing human ACE2, human embryonic kidney 293T/17 cells were transfected with pcDNA3.1(-)hACE2 (Addgene plasmid #1786). Transfection was performed in 293T/17 cells using the genejuice (Novagen, USA) transfection kit according to manufacturer's protocol. At 24h post-transfection, cells were washed with phosphate-buffered saline (PBS) and cultured for recovering at 37C for 24h in Dulbecco's MEM supplemented with 10% heat-inactivated fetal calf serum (FCS), L-glutamine and penicillin/streptomycin (10 U/ml) After 24h of recovery, cells were cultured in media supplemented with G418 (5mg/mL) (Thermo Fisher) and passage for 3 weeks at 37C. Surviving clones were analyzed for ACE2 expression via flow cytometry and PCR.

Virus binding and sensitive p24 ELISA

In order to determine SARS-CoV-2 binding, target cells were exposed to 95 ng of pseudotyped SARS-CoV-2 virus for 4 hours at 4°C. Cells were washed to remove the unbound virus and lysed with lysis buffer. Binding and internalization was quantified by RETRO-TEK HIV-1 p24 ELISA according to manufacturer instructions (ZeptoMetrix Corporation).

Infection assays

HuH7.5, 293T(+hACE2) and undifferentiated Caco2 were exposed to 95 ng of pseudotyped SARS-CoV-2 and polarized Caco2 cells to 477.62 ng of pseudotyped SARS-CoV-2. Virus was pre-incubated with 250U LMWH or UF heparin prior to addition of cells. Infection was measured after 5 days at 37°C by the Luciferase assay system (Promega, USA) according to manufacturer's instructions.

Primary human cells

CD14+ monocytes were isolated from the blood of healthy volunteer donors (Sanquin blood bank) and subsequently differentiated into monocyte-derived DCs as described previously (60). Epidermal sheets were prepared as described previously (39, 40). Briefly, skin-grafts were obtained using a dermatome (Zimmer Biomet, Indiana USA). After

373 incubation with Dispase II (1 U/ml, Roche Diagnostics), epidermal sheets were separated
374 from dermis, washed and cultured in IMDM (Thermo Fischer Scientific, USA)
375 supplemented with 10% FCS, gentamycine (20 µg/ml, Centrafarm, Netherlands),
376 pencilline/streptomycin (10 U/ml and 10 µg/ml, respectively; Invitrogen) for 3 days after
377 which LCs were harvested. Purity of LCs was routinely verified by flow cytometry using
378 antibodies directed against CD207 (langerin) and CD1a.
379 Alveolar macrophages were prepared from broncheo-alveolar lavage (BAL) fluid that was
380 obtained as spare material from the ongoing DIVA study (Netherlands Trial Register:
381 NL6318; AMC Medical Ethical Committee approval number: 2014_294). The DIVA study
382 includes healthy male volunteers aged 18-35. In this study, the subjects are given a first
383 hit of lipopolysaccharide (LPS) and, two hours later, a second hit of either fresh or aged
384 platelet concentrate or NaCl 0.9%. Six hours after the second hit, a BAL is performed by
385 a trained pulmonologist according to national guidelines. Fractions 2-8 are pooled and
386 split in two, one half is centrifuged (4 °C, 1750 G, 10 min.), the cell pellet of which was
387 used in this research. Since the COVID-19 pandemic, subjects are also screened for
388 SARS-CoV-2 (via throat swab PCR) 2 days prior to the BAL. All subjects in the DIVA study
389 have signed an informed consent form. Cells were washed and plated. After two hours the
390 wells were washed to remove non-adherent cells and adherent macrophages were
391 infected.
392
393 *Transmission assays and co-culture*
394 Alveolar macrophages, DCs or LCs were exposed to 191.05 ng of pseudotyped SARS-
395 CoV-2 or pseudotyped SARS-CoV-2 pre-incubated with 250U UF heparin or LMWH for 4
396 hours, harvested, extensively washed to remove unbound virus and co-cultured with
397 Huh7.5 for 5 days at 37°C after which they were analyzed for with the Luciferase assay
398 system (Promega, USA) according to manufacturer's instructions.
399
400 *RNA isolation and quantitative real-time PCR*
401 mRNA was isolated with an mRNA Capture kit (Roche) and cDNA was synthesized with
402 a reverse-transcriptase kit (Promega) and PCR amplification was performed in the
403 presence of SYBR green in a 7500 Fast Realtime PCR System (ABI). Specific primers
404 were designed with Primer Express 2.0 (Applied Biosystems). Primer sequences used for
405 mRNA expression were for gene product: GAPDH, forward primer

(CCATGTTCGTCATGGGTGTG), reverse primer (GGTGCTAA GCAGTTGGTGGTG). For gene product: ACE2, forward primer (GGACCCAGGAAATGTTCAGA), reverse primer (GGCTGCAGAAAGTGACATGA). For gene product: Syndecan 1, forward primer (ATCACCTTGTCACAGCAGACCC) reverse primer (CTCCACTTCTGGCAGGACTACA). Syndecan 4, forward primer (AGGTGTCAATGTCCAGCACTGTG) reverse primer (AGCAGTAGGATCAGGAAGACGGC). The normalized amount of target mRNA was calculated from the Ct values obtained for both target and household mRNA with the equation Nt = 2Ct(GAPDH) − Ct(target). For relative mRNA expression, control siRNA sample was set at 1 for each donor.

RNA interference

Huh7.5 cells were silenced by electroporation with Neon Transfection System (Thermo Fischer Scientific) according to the manufacturers protocol The siRNA (SMARTpool; Dharmacon) were specific for Syndecan 1 (10 µM siRNA, M-010621-01-0005, SMARTpool; Dharmacon), Syndecan 4 (10 µM siRNA, M-003706-01-0005, SMARTpool; Dharmacon) whereas non-targeting siRNA (D-001206-13, SMARTpool; Dharmacon) served as control. Cells were used for experiments 48 hours after silencing and silencing efficiency of the specific targets was verified by real-time PCR and flow cytometry.

Biosynthesis inhibition and enzymatic treatment

HuH7.5 cells were treated in D-PBS/0.25% BSA with 46 miliunits heparinase III (Amsbio) for 1 hour at 37°C, washed and used in subsequent experiments. Enzymatic digestion was verified by flow cytometry using antibodies directed against heparan sulfates and digested heparan sulfates.

Statistics

A two-tailed, parametric Student's *t*-test for paired observations (differences within the same donor) or unpaired observation (differences between different donors) was performed. For unpaired, non-parametric observations a one-way ANOVA or two-way ANOVA test were performed. Statistical analyses were performed using GraphPad Prism 8 software and significance was set at *P< 0.05, **P<0.01***P<0.001****P<0.0001.

Study approval

This study was performed according to the Amsterdam University Medical Centers, location AMC Medical Ethics Committee guidelines and all donors for blood, skin and BAL gave written informed consent in accordance with the Declaration of Helsinki.

Author Contributions

M.B-J and J.E conceived and designed experiments; M.B-J, J.E, T.M.K, L.C.H, J.L.v.H performed the experiments and contributed to scientific discussion; P.J.M.B., G.J.d.B, R.W.S., M.J.v.G, B.M.N and N.A.K contributed essential research materials and scientific input. M.B-J, J.E, T.M.K and T.B.H.G analyzed and interpreted data; J.E, M.B-J and T.B.H.G. wrote the manuscript with input from all listed authors. T.B.H.G. was involved in all aspects of the study.

Acknowledgements

We thank Jonne Snitselaar and Yoann Aldon for help with production of antibodies and Rene Jonkers and Peter Bonta for conducting the BAL.

Funding

This research was funded by the European Research Council (Advanced grant 670424 to T.B.H.G.), Amsterdam UMC PhD grant and two COVID-19 grants from the Amsterdam institute for Infection & Immunity (to T.B.H.G., R.W.S. and M.J.v.G.). This study was also supported by the Netherlands Organization for Scientific Research (NWO) through a Vici grant (to R.W.S.), and by the Bill & Melinda Gates Foundation through the Collaboration for AIDS Vaccine Discovery (CAVD), grant INV-002022 (to R.W.S.).

Competing interests

There have no conflicts of interest.

Data and materials availability

Reagents and materials presented in this study are available from the corresponding authors under a MTA with the Amsterdam UMC.

References

1. P. Zhou *et al.*, A pneumonia outbreak associated with a new coronavirus of probable bat origin. *Nature* **579**, 270-273 (2020).
2. K. Yuki, M. Fujiogi, S. Koutsogiannaki, COVID-19 pathophysiology: A review. *Clin Immunol* **215**, 108427 (2020).
3. N. Zhu *et al.*, A Novel Coronavirus from Patients with Pneumonia in China, 2019. *N Engl J Med* **382**, 727-733 (2020).
4. M. Nicola *et al.*, The socio-economic implications of the coronavirus pandemic (COVID-19): A review. *Int J Surg* **78**, 185-193 (2020).
5. World Health Organization (2020) Timeline of WHO's response to COVID-19.
6. H. Harapan *et al.*, Coronavirus disease 2019 (COVID-19): A literature review. *J Infect Public Health* **13**, 667-673 (2020).
7. M. Ferioli *et al.*, Protecting healthcare workers from SARS-CoV-2 infection: practical indications. *Eur Respir Rev* **29** (2020).
8. J. S. Peiris, K. Y. Yuen, A. D. Osterhaus, K. Stöhr, The severe acute respiratory syndrome. *N Engl J Med* **349**, 2431-2441 (2003).
9. K. P. Y. Hui *et al.*, Tropism, replication competence, and innate immune responses of the coronavirus SARS-CoV-2 in human respiratory tract and conjunctiva: an analysis in ex-vivo and in-vitro cultures. *Lancet Respir Med* 10.1016/s2213-2600(20)30193-4 (2020).
10. M. M. Lamers *et al.*, SARS-CoV-2 productively infects human gut enterocytes. *Science* 10.1126/science.abc1669 (2020).
11. L. Wright, A. Steptoe, D. Fancourt, Are we all in this together? Longitudinal assessment of cumulative adversities by socioeconomic position in the first 3 weeks of lockdown in the UK. *J Epidemiol Community Health* 10.1136/jech-2020-214475 (2020).
12. S. K. Brooks *et al.*, The psychological impact of quarantine and how to reduce it: rapid review of the evidence. *Lancet* **395**, 912-920 (2020).
13. M. Letko, A. Marzi, V. Munster, Functional assessment of cell entry and receptor usage for SARS-CoV-2 and other lineage B betacoronaviruses. *Nat Microbiol* **5**, 562-569 (2020).
14. R. J. Hulswit, C. A. de Haan, B. J. Bosch, Coronavirus Spike Protein and Tropism Changes. *Adv Virus Res* **96**, 29-57 (2016).
15. B. J. Bosch, R. van der Zee, C. A. de Haan, P. J. Rottier, The coronavirus spike protein is a class I virus fusion protein: structural and functional characterization of the fusion core complex. *J Virol* **77**, 8801-8811 (2003).
16. F. Li, W. Li, M. Farzan, S. C. Harrison, Structure of SARS coronavirus spike receptor-binding domain complexed with receptor. *Science* **309**, 1864-1868 (2005).
17. N. Wang *et al.*, Structure of MERS-CoV spike receptor-binding domain complexed with human receptor DPP4. *Cell Res* **23**, 986-993 (2013).
18. C. Burkard *et al.*, Coronavirus cell entry occurs through the endo-/lysosomal pathway in a proteolysis-dependent manner. *PLoS Pathog* **10**, e1004502 (2014).
19. S. Xia *et al.*, Inhibition of SARS-CoV-2 (previously 2019-nCoV) infection by a highly potent pan-coronavirus fusion inhibitor targeting its spike protein that harbors a high capacity to mediate membrane fusion. *Cell Res* **30**, 343-355 (2020).
20. M. Hoffmann *et al.*, SARS-CoV-2 Cell Entry Depends on ACE2 and TMPRSS2 and Is Blocked by a Clinically Proven Protease Inhibitor. *Cell* **181**, 271-280.e278 (2020).

21. I. Hamming *et al.*, Tissue distribution of ACE2 protein, the functional receptor for SARS coronavirus. A first step in understanding SARS pathogenesis. *J Pathol* **203**, 631-637 (2004).
22. X. Zou *et al.*, Single-cell RNA-seq data analysis on the receptor ACE2 expression reveals the potential risk of different human organs vulnerable to 2019-nCoV infection. *Front Med* **14**, 185-192 (2020).
23. P. J. M. Brouwer *et al.*, Potent neutralizing antibodies from COVID-19 patients define multiple targets of vulnerability. *Science* **369**, 643-650 (2020).
24. G. Roderiquez *et al.*, Mediation of human immunodeficiency virus type 1 binding by interaction of cell surface heparan sulfate proteoglycans with the V3 region of envelope gp120-gp41. *J Virol* **69**, 2233-2239 (1995).
25. A. Milewska *et al.*, Human coronavirus NL63 utilizes heparan sulfate proteoglycans for attachment to target cells. *J Virol* **88**, 13221-13230 (2014).
26. J. Jiang *et al.*, Hepatitis C virus attachment mediated by apolipoprotein E binding to cell surface heparan sulfate. *J Virol* **86**, 7256-7267 (2012).
27. A. P. Byrnes, D. E. Griffin, Binding of Sindbis virus to cell surface heparan sulfate. *J Virol* **72**, 7349-7356 (1998).
28. B. M. Nijmeijer *et al.*, Syndecan 4 Upregulation on Activated Langerhans Cells Counteracts Langerin Restriction to Facilitate Hepatitis C Virus Transmission. *Front Immunol* **11**, 503 (2020).
29. A. K. Kakkar, Low- and ultra-low-molecular-weight heparins. *Best Pract Res Clin Haematol* **17**, 77-87 (2004).
30. N. Tang *et al.*, Anticoagulant treatment is associated with decreased mortality in severe coronavirus disease 2019 patients with coagulopathy. *J Thromb Haemost* **18**, 1094-1099 (2020).
31. G. J. Merli, J. B. Groce, Pharmacological and clinical differences between low-molecular-weight heparins: implications for prescribing practice and therapeutic interchange. *P t* **35**, 95-105 (2010).
32. Q. Wang *et al.*, Structural and Functional Basis of SARS-CoV-2 Entry by Using Human ACE2. *Cell* **181**, 894-904.e899 (2020).
33. H. Zhang, J. M. Penninger, Y. Li, N. Zhong, A. S. Slutsky, Angiotensin-converting enzyme 2 (ACE2) as a SARS-CoV-2 receptor: molecular mechanisms and potential therapeutic target. *Intensive Care Med* **46**, 586-590 (2020).
34. H. P. Jia *et al.*, ACE2 receptor expression and severe acute respiratory syndrome coronavirus infection depend on differentiation of human airway epithelia. *J Virol* **79**, 14614-14621 (2005).
35. H. Chu *et al.*, Comparative replication and immune activation profiles of SARS-CoV-2 and SARS-CoV in human lungs: an ex vivo study with implications for the pathogenesis of COVID-19. *Clin Infect Dis* 10.1093/cid/ciaa410 (2020).
36. K. S. Jones, C. Petrow-Sadowski, Y. K. Huang, D. C. Bertolette, F. W. Ruscetti, Cell-free HTLV-1 infects dendritic cells leading to transmission and transformation of CD4(+) T cells. *Nat Med* **14**, 429-436 (2008).
37. C. M. Ribeiro *et al.*, Receptor usage dictates HIV-1 restriction by human TRIM5α in dendritic cell subsets. *Nature* **540**, 448-452 (2016).

38. A. Marzi *et al.*, DC-SIGN and DC-SIGNR interact with the glycoprotein of Marburg virus and the S protein of severe acute respiratory syndrome coronavirus. *J Virol* **78**, 12090-12095 (2004).
39. L. de Witte *et al.*, Langerin is a natural barrier to HIV-1 transmission by Langerhans cells. *Nat Med* **13**, 367-371 (2007).
40. R. Sarrami-Forooshani *et al.*, Human immature Langerhans cells restrict CXCR4-using HIV-1 transmission. *Retrovirology* **11**, 52 (2014).
41. M. Merad, F. Ginhoux, M. Collin, Origin, homeostasis and function of Langerhans cells and other langerin-expressing dendritic cells. *Nat Rev Immunol* **8**, 935-947 (2008).
42. T. B. Geijtenbeek *et al.*, DC-SIGN, a dendritic cell-specific HIV-1-binding protein that enhances trans-infection of T cells. *Cell* **100**, 587-597 (2000).
43. S. Bacsa *et al.*, Syndecan-1 and syndecan-2 play key roles in herpes simplex virus type-1 infection. *J Gen Virol* **92**, 733-743 (2011).
44. K. Hayashida, D. R. Johnston, O. Goldberger, P. W. Park, Syndecan-1 expression in epithelial cells is induced by transforming growth factor beta through a PKA-dependent pathway. *J Biol Chem* **281**, 24365-24374 (2006).
45. Y. H. Teng, R. S. Aquino, P. W. Park, Molecular functions of syndecan-1 in disease. *Matrix Biol* **31**, 3-16 (2012).
46. C. Mycroft-West *et al.*, The 2019 coronavirus (SARS-CoV-2) surface protein (Spike) S1 Receptor Binding Domain undergoes conformational change upon heparin binding. http://dx.doi.org/10.1101/2020.02.29.971093.
47. L. J. Partridge, L. R. Green, P. N. Monk, Unfractionated heparin potently inhibits the binding of SARS-CoV-2 spike protein to a human cell line. http://dx.doi.org/10.1101/2020.05.21.107870.
48. L. Liu *et al.*, SARS-CoV-2 spike protein binds heparan sulfate in a length- and sequence-dependent manner. http://dx.doi.org/10.1101/2020.05.10.087288.
49. H. Li *et al.*, SARS-CoV-2 and viral sepsis: observations and hypotheses. *Lancet* **395**, 1517-1520 (2020).
50. G. J. Randolph, V. Angeli, M. A. Swartz, Dendritic-cell trafficking to lymph nodes through lymphatic vessels. *Nat Rev Immunol* **5**, 617-628 (2005).
51. L. Wu, V. N. KewalRamani, Dendritic-cell interactions with HIV: infection and viral dissemination. *Nat Rev Immunol* **6**, 859-868 (2006).
52. C. Chute *et al.*, Syndecan-1 induction in lung microenvironment supports the establishment of breast tumor metastases. *Breast Cancer Res* **20**, 66 (2018).
53. Q. Shi, J. Jiang, G. Luo, Syndecan-1 serves as the major receptor for attachment of hepatitis C virus to the surfaces of hepatocytes. *J Virol* **87**, 6866-6875 (2013).
54. L. de Witte *et al.*, Syndecan-3 is a dendritic cell-specific attachment receptor for HIV-1. *Proc Natl Acad Sci U S A* **104**, 19464-19469 (2007).
55. Z. Zhai *et al.*, Prevention and Treatment of Venous Thromboembolism Associated with Coronavirus Disease 2019 Infection: A Consensus Statement before Guidelines. *Thromb Haemost* **120**, 937-948 (2020).
56. World Health Organization (2020) Clinical management of COVID-19. Interim guidance 27 May 2020. (World Health Organization), p 62.
57. Z. Zhang, C. Coomans, G. David, Membrane heparan sulfate proteoglycan-supported FGF2-FGFR1 signaling: evidence in support of the "cooperative end structures" model. *J Biol Chem* **276**, 41921-41929 (2001).

58. B. D. Lindenbach *et al.*, Complete replication of hepatitis C virus in cell culture. *Science* **309**, 623-626 (2005).
59. Y. Aldon *et al.*, Rational Design of DNA-Expressed Stabilized Native-Like HIV-1 Envelope Trimers. *Cell Rep* **24**, 3324-3338.e3325 (2018).
60. A. W. Mesman *et al.*, Measles virus suppresses RIG-I-like receptor activation in dendritic cells via DC-SIGN-mediated inhibition of PP1 phosphatases. *Cell Host Microbe* **16**, 31-42 (2014).

615 **Figures 1 to 6**

616 **Figure 1**

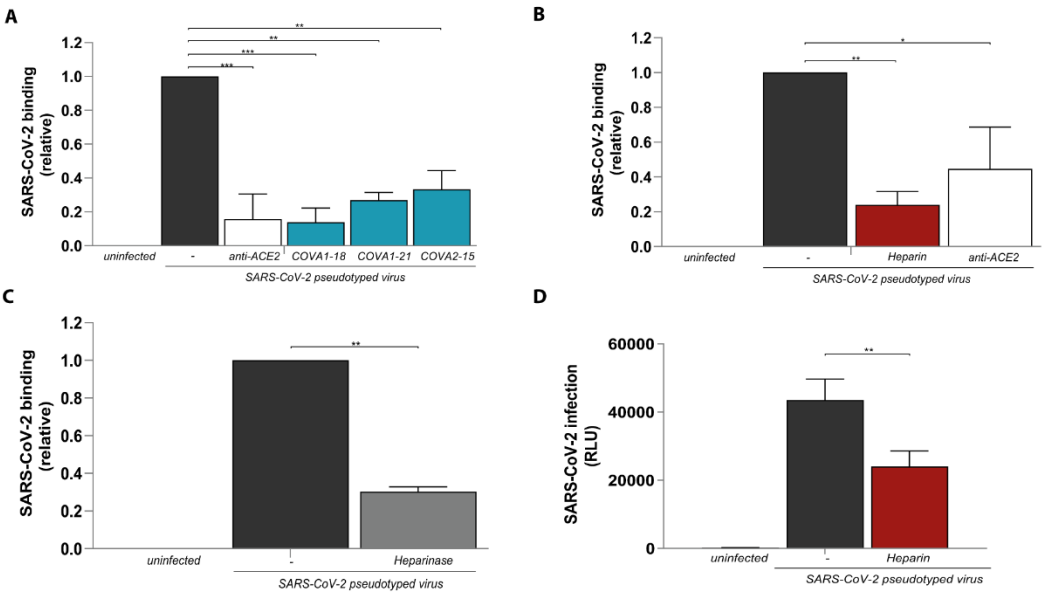

Figure 1. Heparan sulfates are crucial for SARS-CoV-2 binding and infection.
(**A-B**) Huh 7.5 cells were preincubated with neutralizing antibody to ACE2 and SARS-CoV-2 pseudovirus was pre-incubated with mAb COVA1-18, COVA1-21 and COVA2-15 or UF heparin (250IU). Cells were infected with SARS-CoV-2 pseudovirus and binding was determined by ELISA. (**C**) Heparan sulfates were removed from Huh 7.5 cells by heparinase treatment and SARS-CoV-2 pseudovirus binding was determined. Error bars are the mean ± SEM from three independent experiments. (**D**) Huh 7.5 cells were infected with SARS-CoV-2 pseudovirus and infection was measured after 5 days of culture by luciferase assay. Virus was pretreated with heparin (250IU). Data show the mean values and error bars are the SEM. Statistical analysis was performed using (**A**) ordinary one-way ANOVA with Tukey multiple-comparison test. ***p= 0.0006, ***p= 0.0005, **p= 0.0018, **p= 0.0036 (n = 3), (**B**) **p= 0.0010, *p= 0.0255 (n=4), (**C**) two-tailed, unpaired Student's t-test with Welch's correction. **p= 0.0012 (n = 3), (**D**) ordinary one-way ANOVA with Tukey multiple-comparison test. **p= 0.0085 (n=6 measured in triplicate). RLU: relative light units.

617

618

Figure 2

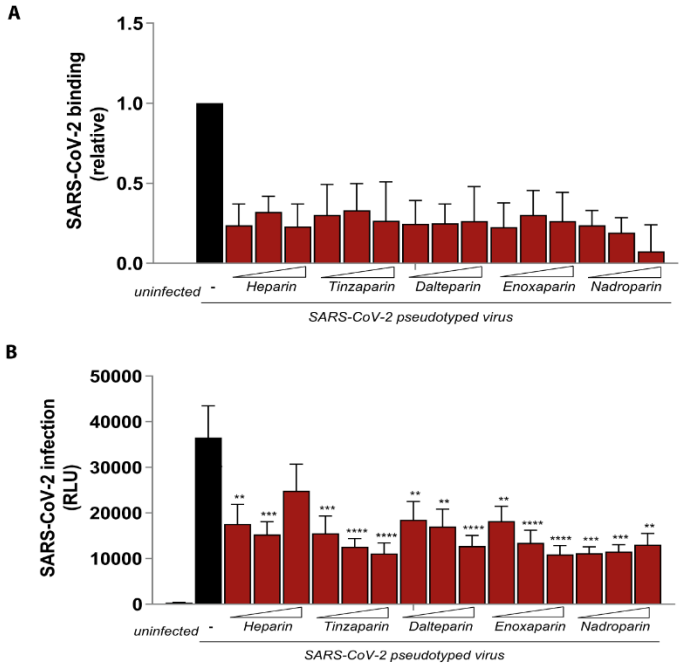

Figure 2. LMWH block binding and infection by SARS-CoV-2.
SARS-CoV-2 was pretreated with UF heparin and different LMWH at different concentrations (50-100-250IU) and (**A**) binding to Huh 7.5 cells was determined or (**B**) infection was measured after 5 days by ELISA or luciferase assay, respectively. Data show the mean values and error bars are the SEM. Statistical analysis was performed using (**A**) ordinary one-way ANOVA with Tukey's multiple-comparison test. (n = 3), (**B**) ordinary one-way ANOVA with Dunnett's multiple-comparison test. **p= 0.0018, ***p= 0.0003, ***p= 0.0004, ****p< 0.0001, **p= 0.0036, **p= 0.0012, **p= 0.0029 (n = 3 donors measured in triplicate). RLU: relative light units.

623 **Figure 3**

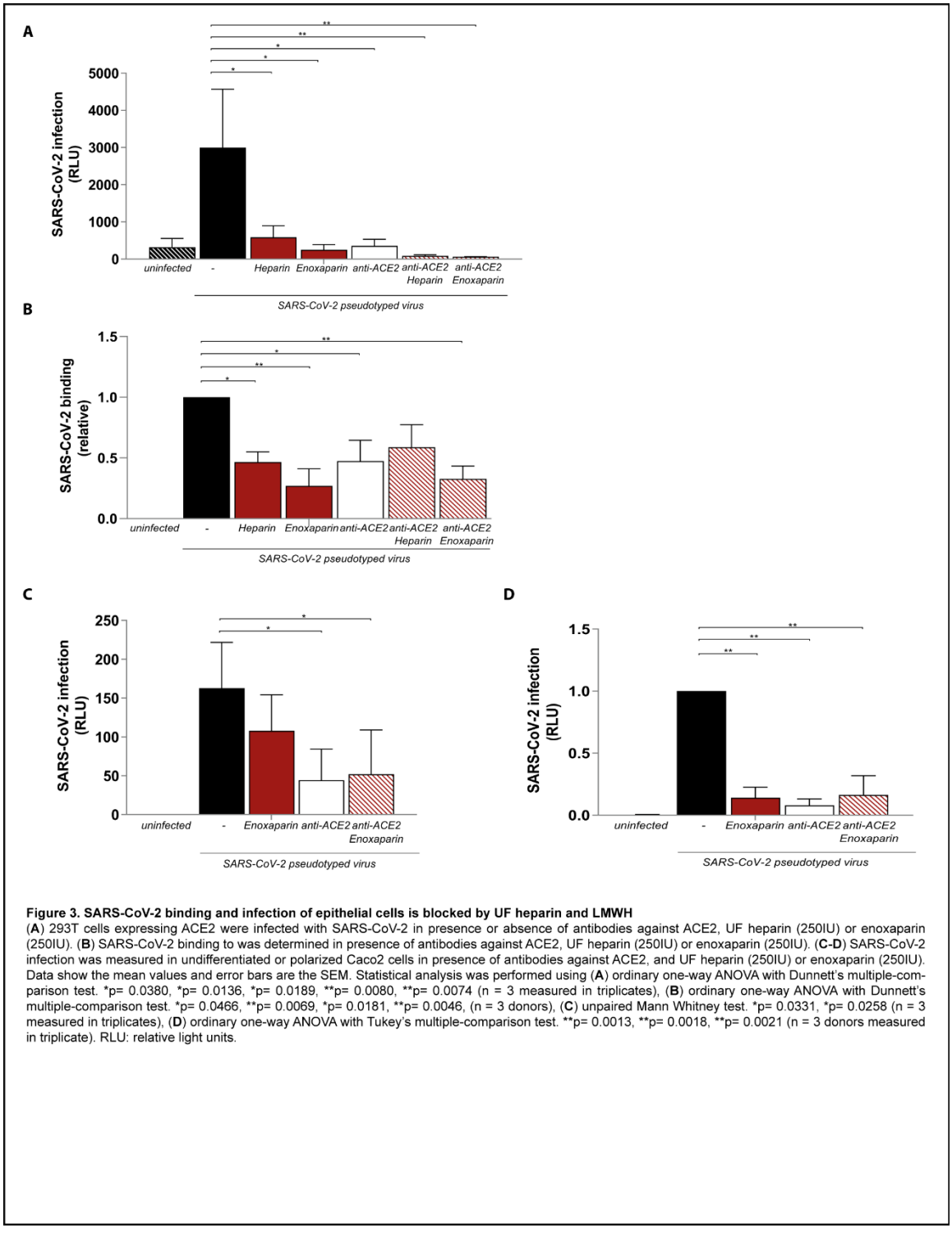

Figure 3. SARS-CoV-2 binding and infection of epithelial cells is blocked by UF heparin and LMWH
(**A**) 293T cells expressing ACE2 were infected with SARS-CoV-2 in presence or absence of antibodies against ACE2, UF heparin (250IU) or enoxaparin (250IU). (**B**) SARS-CoV-2 binding to was determined in presence of antibodies against ACE2, UF heparin (250IU) or enoxaparin (250IU). (**C-D**) SARS-CoV-2 infection was measured in undifferentiated or polarized Caco2 cells in presence of antibodies against ACE2, and UF heparin (250IU) or enoxaparin (250IU). Data show the mean values and error bars are the SEM. Statistical analysis was performed using (**A**) ordinary one-way ANOVA with Dunnett's multiple-comparison test. *p= 0.0380, *p= 0.0136, *p= 0.0189, **p= 0.0080, **p= 0.0074 (n = 3 measured in triplicates), (**B**) ordinary one-way ANOVA with Dunnett's multiple-comparison test. *p= 0.0466, **p= 0.0069, *p= 0.0181, **p= 0.0046, (n = 3 donors), (**C**) unpaired Mann Whitney test. *p= 0.0331, *p= 0.0258 (n = 3 measured in triplicates), (**D**) ordinary one-way ANOVA with Tukey's multiple-comparison test. **p= 0.0013, **p= 0.0018, **p= 0.0021 (n = 3 donors measured in triplicate). RLU: relative light units.

624

625

626 **Figure 4**

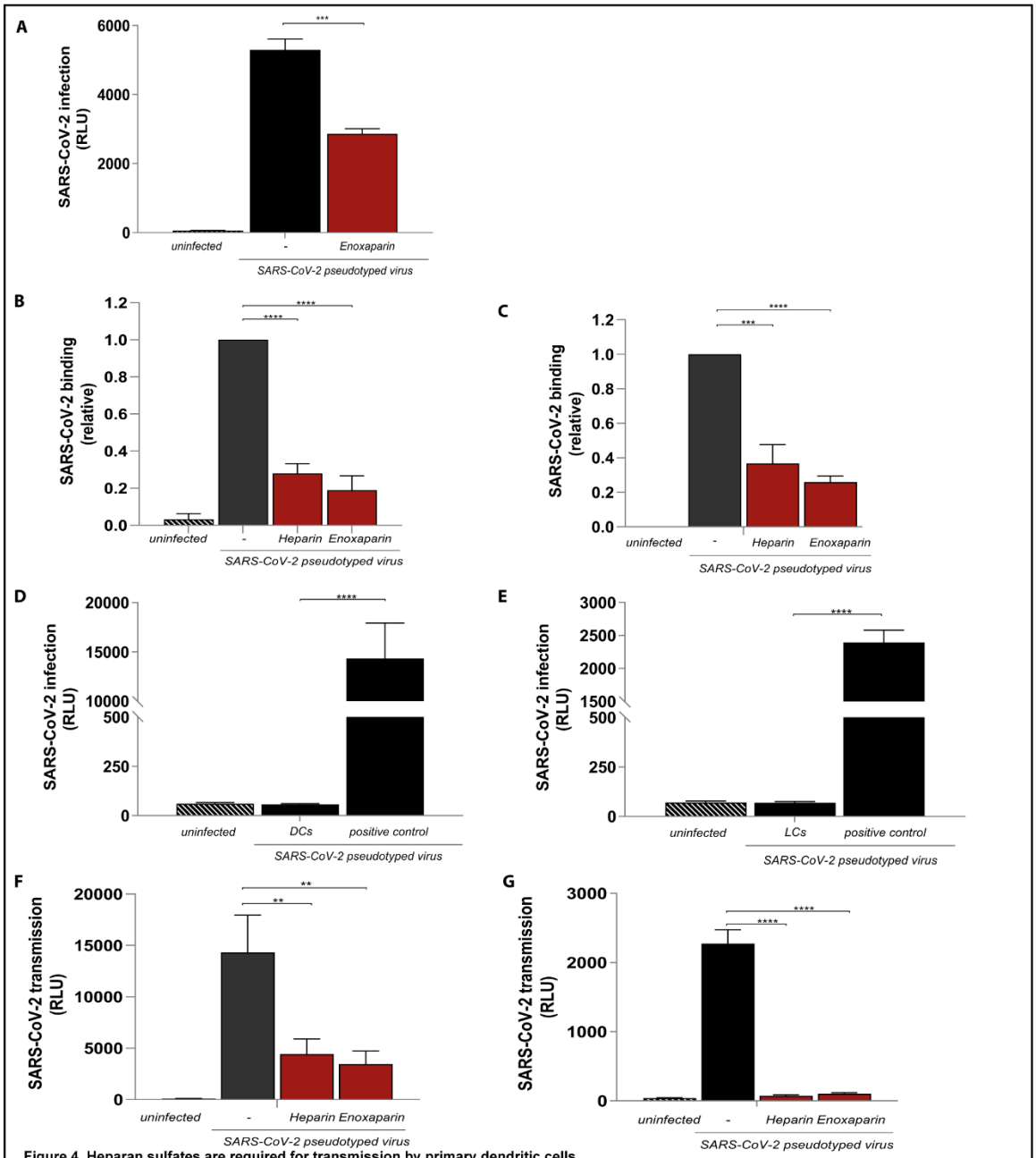

Figure 4. Heparan sulfates are required for transmission by primary dendritic cells.
(**A**) Alveolar macrophages (BAL) infected with SARS-CoV-2 and infection was measured after 5 days. One representative donor out of 3 is depicted. (**B-C**) SARS-CoV-2 binding to monocyte-derived DCs (**B**) and primary LCs (**C**) in presence of UF heparin (250IU) or enoxaparin (250IU). (**D-E**) DCs (**D**) and LCs (**E**) were infected with SARS-CoV-2 and infection was measured after 5 days. As positive controls Huh 7.5 cells were infected. (**F-G**) DCs (**F**) and LCs (**G**) were preincubated with SARS-CoV-2 pseudovirus for 4 h in presence or absence of UF heparin (250 IU) or enoxaparin (250 IU), extensively washed and co-cultured with Huh 7.5 cells. Transmission by DCs or LCs to Huh 7.5 cells was determined by luciferase assay. Data show the mean values and error bars are the SEM. Statistical analysis was performed using (**A**) ordinary one-way ANOVA with Tukey's multiple-comparison test. ***p= 0.0004 (n = 1), (**B-C**) ordinary one-way ANOVA with Tukey's multiple-comparison test. (**B**)****p< 0.0001, (**C**) ***p= 0.0002, ****p< 0.0001 (n = 4), (**D-E**) ordinary one-way ANOVA with Tukey's multiple-comparison test. ****p< 0.0001 (**D**) n=4 measured in triplicate and (**E**) n = 3 donors measured in duplicate, (**F**) ordinary one-way ANOVA with Dunnett's multiple-comparison test. **p= 0.0042, **p= 0.0016 (n = 4 measured in triplicate), (**G**) ordinary one-way ANOVA with Tukey's multiple-comparison test.)****p< 0.0001 (n = 3 measured in triplicate). DCs: Dendritic cells, LCs: Langerhans cells, RLU: relative light units.

627

628

Figure 5

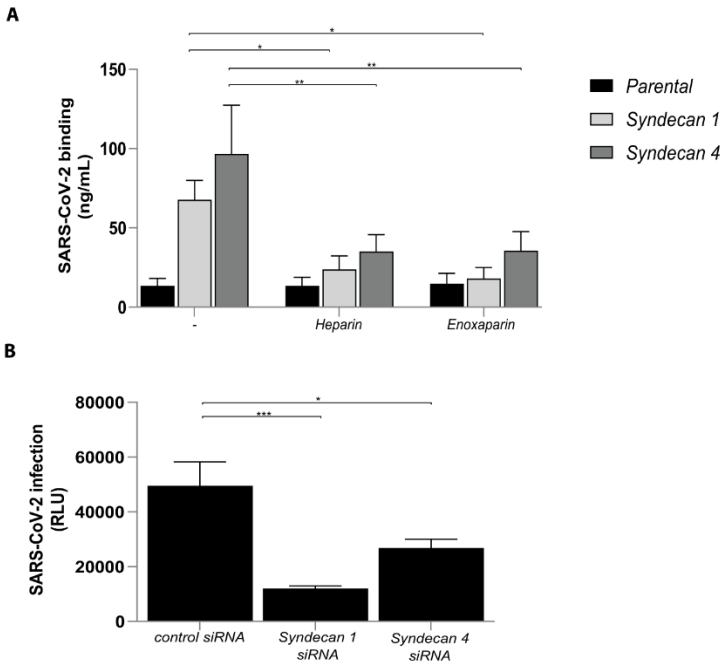

Figure 5. Heparan sulfate proteoglycans Syndecan 1 and 4 are important for SARS-CoV-2 binding and infection
(**A**) Namalwa cells ectopically expressing either Syndecan 1 or 4 were exposed to SARS-CoV-2 pseudovirus, in presence or absence of UF heparin (250IU) or enoxaparin (250IU and binding was measured after 4h. (**B**) Syndecan 1 and 4 were silenced by RNA interference in Huh7.5 cells and infection with SARS-CoV-2 pseudovirus was measured after 5 days. Representative data for an experiment repeated more than three times with similar results. Data show the mean values and error bars are the SEM. Statistical analysis was performed using (**A**) 2way-ANOVA with Dunnett's multiple-comparison test. *p= 0.0408, *p= 0.0189, **p= 0.0032, **p= 0.0035 (n = 7), (**B**) 2way-ANOVA with Tukey's multiple-comparison test. ***p= 0.0002, *p= 0.0124. (n = 1 measured in triplicate). siRNA: RNA interference, RLU: relative light units.

632 **Figure 6**

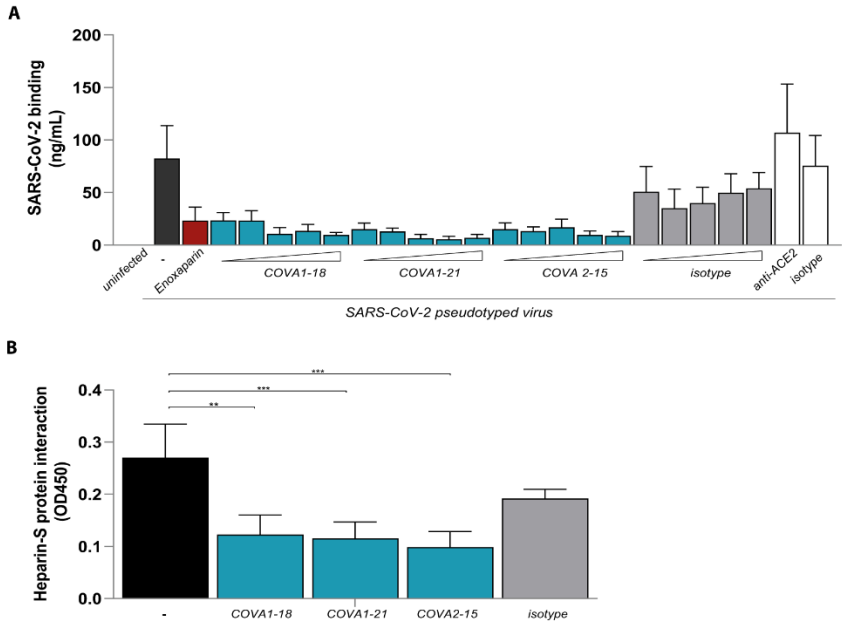

Figure 6. Neutralizing antibodies against SARS-CoV-2 block heparan sulfate binding.
(**A**) SARS-CoV-2 pseudovirus was treated with neutralizing antibodies against SARS-CoV-2 (COVA1-18, COVA1-21 and COVA2-15) and isotype control (VRC01 in grey) at concentrations 0.05, 0.1, 0.5, 1 and 5 µg/mL, while Syndecan 1 expressing Namalwa cells were preincubated with anti-ACE2 antibody and it corresponding isotype (both in white). Binding was determined by ELISA. (**B**) The ability of the neutralizing antibodies to prevent SARS-CoV-2 S protein binding to heparan sulfates was measured in the Heparin-SARS-CoV-2 S protein binding assay. S protein was preincubated with the different neutralizing antibodies (COVA1-18, COVA1-21 and COVA2-15) and isotype control (VRC01) and binding was determined. Data show the mean values and error bars are the SEM. Statistical analysis was performed using (**A**) ordinary one-way ANOVA with Tukey's multiple-comparison test. (n = 3), (**B**) 2way-ANOVA with Tukey's multiple-comparison test. **p= 0.0019, ***p= 0.0010, ***p= 0.0002. (n = 2 measured in duplicates).

633

634

635

Supplementary Figures 1 to 2

Supplementary Figure 1

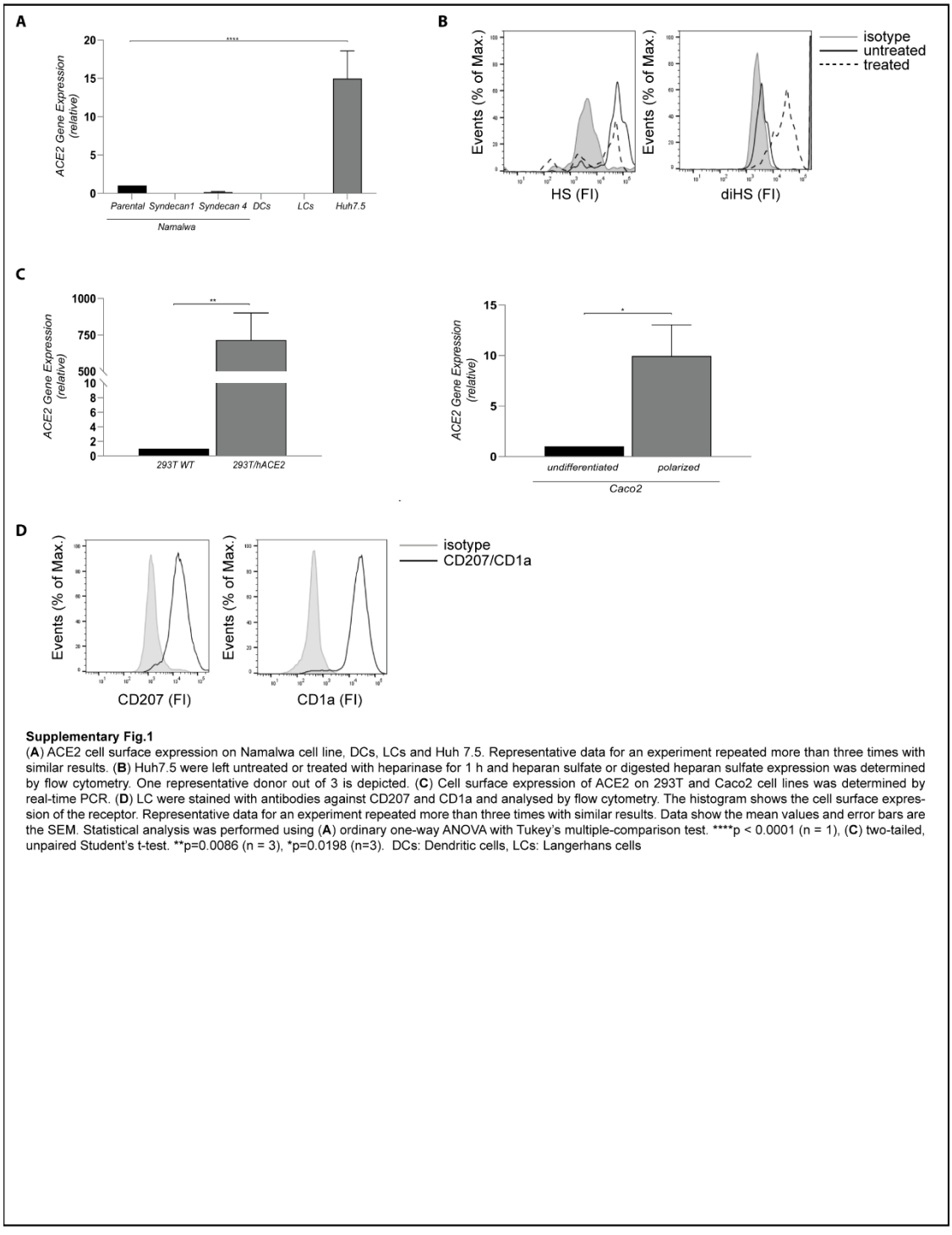

Supplementary Fig.1
(**A**) ACE2 cell surface expression on Namalwa cell line, DCs, LCs and Huh 7.5. Representative data for an experiment repeated more than three times with similar results. (**B**) Huh7.5 were left untreated or treated with heparinase for 1 h and heparan sulfate or digested heparan sulfate expression was determined by flow cytometry. One representative donor out of 3 is depicted. (**C**) Cell surface expression of ACE2 on 293T and Caco2 cell lines was determined by real-time PCR. (**D**) LC were stained with antibodies against CD207 and CD1a and analysed by flow cytometry. The histogram shows the cell surface expression of the receptor. Representative data for an experiment repeated more than three times with similar results. Data show the mean values and error bars are the SEM. Statistical analysis was performed using (**A**) ordinary one-way ANOVA with Tukey's multiple-comparison test. ****p < 0.0001 (n = 1), (**C**) two-tailed, unpaired Student's t-test. **p=0.0086 (n = 3), *p=0.0198 (n=3). DCs: Dendritic cells, LCs: Langerhans cells

Supplementary Figure 2

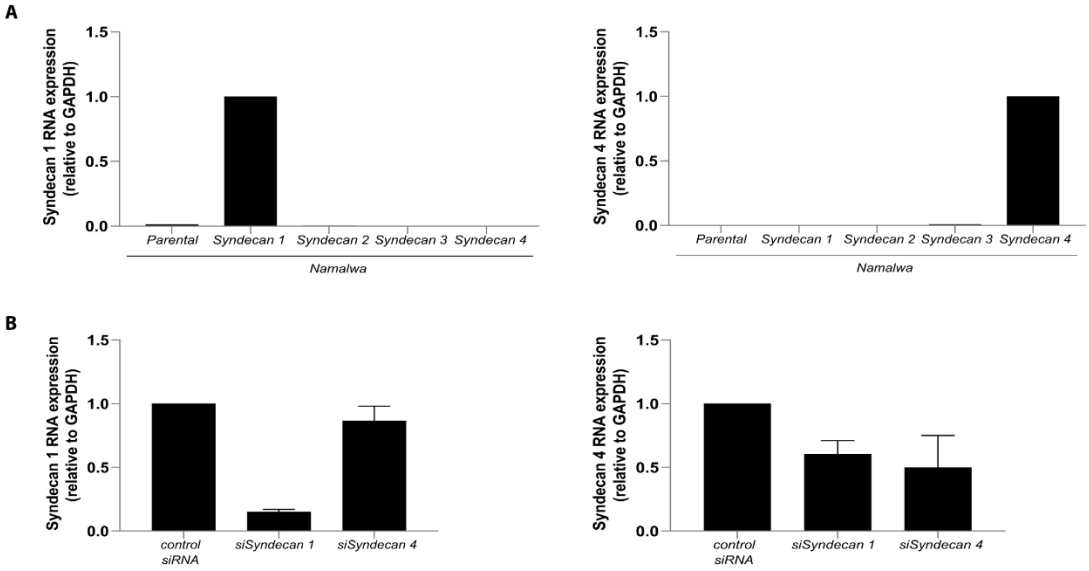

Supplementary Fig.2

(**A**) Different Namalwa Syndecan cell lines express Syndecan 1 - 4, on the cell surface determined by real-time PCR. (**B**) Syndecan 1 and 4 silencing was confirmed by real-time PCR. mRNA expression was normalized to GAPDH and set at 1 in cells treated with control siRNA. Representative data for an experiment repeated more than three times with similar results.

640